HOKKAIDO UNIVERSITY

Title	Time-dependent Hartree-Fock-Bogoliubov method for molecular systems : An alternative excited-state methodology including static electron correlation
Author(s)	Nishida, Masatsugu; Akama, Tomoko; Kobayashi, Masato et al.
Citation	Chemical physics letters, 816, 140386 https://doi.org/10.1016/j.cplett.2023.140386
Issue Date	2024-04
Doc URL	https://hdl.handle.net/2115/95118
Rights	©2023 John Benjamins. You should be contacted to John Benjamins for permission to re-use or reprint the material in any form.
Rights(URL)	https://creativecommons.org/licenses/by-nc-nd/4.0/
Type	journal article
File Information	CPL_nishida_revise_v2.pdf



Hokkaido University Collection of Scholarly and Academic Papers : HUSCAP

Time-dependent Hartree–Fock–Bogoliubov method for molecular systems: An alternative excited-state methodology including static electron correlation

Masatsugu Nishida[1], Tomoko Akama[2], Masato Kobayashi[2,3 a)], and Tetsuya Taketsugu[2,3]

[1]*Graduate School of Chemical Sciences and Engineering, Hokkaido University, Sapporo 060-0810, Japan*

[2]*WPI-ICReDD, Hokkaido University, Sapporo 001-0021, Japan*

[3]*Faculty of Science, Hokkaido University, Sapporo 060-0810, Japan*

[a)]Electronic mail: k-masato@sci.hokudai.ac.jp

Abstract

The Hartree–Fock–Bogoliubov (HFB) method, an efficient way to treat static electron correlations, has been applied to molecular systems in the ground state. In this letter, we propose a time-dependent (TD) HFB method for treating the excited states of molecules with static correlations at a reasonable computational cost. To avoid electron number violations, we also consider the canonical basis variant of the TDHFB method proposed by Ebata *et al.* Results of calculations for the elongated hydrogen molecule reveal that the TDHFB method can partially incorporate two-electron excited determinants.

I. Introduction

An accurate evaluation of excitation energies for molecules is challenging because it requires the description of both ground and excited states having different correlation energies with similar accuracy. If the ground state of the target system has a large static correlation energy (e.g., bond-dissociated molecules and transition-metal compounds), a multi-configurational wavefunction is required for the qualitative description. The most popular method for such a system is the active space-based self-consistent field (SCF) method, which is typified by state-averaged complete active space SCF (SA-CASSCF)[1,2]. However, the scope of its application is limited because its computational cost increases with the size of the active space. In addition, users must set an appropriate active space to maintain accurate results at affordable computational costs. The density matrix renormalization group has been developed[3–5] and has enabled the treatment of a large active space; however, black-box treatment remains difficult[6].

Another approach is geminal-based wavefunction theories[7,8]. In this method, the *N*-electron wavefunction is represented as the antisymmetric product of two-electron wavefunctions called geminals, rather than the one-electron wavefunctions called orbitals. This method can cover a large static correlation energy because each geminal can fully describe the intra-geminal electron correlation. In addition, the computational scaling of practical geminal-based methods is $O(n^3–n^5)$[9,10]. Thus, this method can efficiently construct the *N*-electron wavefunction by incorporating static electron correlation with a lower computational cost than the active-space scheme. Several variants of the geminal-based methods have been proposed both for ground [11–16] and excited [17–20] state calculations.

Here, we focus on the Hartree–Fock–Bogoliubov (HFB) method[21,22]. The HFB method originates from the fusion of the Hartree–Fock (HF) theory and Bardeen–Cooper–Schrieffer theory[23] in superconductivity. It describes the static correlation by considering quasi-particles, which are formally related to geminals. Number-projection associates the HFB theory with the geminal-based wavefunction, which is called antisymmetrized geminal power[24–26]. In the HFB scheme, both the electron and quasi-particle describe the electronic distribution and Hamiltonian. The dimension of the Hamiltonian that must be diagonalized is only twice that of HF. Thus, the HFB method enables the treatment of the static correlation with mean-field computational cost. The HFB method has been highly successful in nuclear physics and superconductivity. In 2002, Staroverov and Scuseria[27] applied this to molecular systems. They found that the HFB energy functional was identical to the corrected HF density matrix functional proposed by Csányi and Arias[28], except for the sign of the correlation term. It indicates that the HFB method is also related to the density

matrix functional theory (DMFT)[29]. They demonstrated that the HFB wavefunction can qualitatively describe strongly correlated systems. However, the HFB wavefunction breaks the electron number conservation, which can be avoided by introducing a chemical potential in the sense that the expectation value of the electron number can be conserved. Although several electron correlation theories based on the HFB concept have been developed and applied to molecular systems[10,30–34], their extension to the excited state remains a frontier[17,18], whereas the time-dependent version of related DMFT has been proposed[35,36].

The excited-state calculation based on the HFB method, which is the time-dependent HFB (TDHFB) method[21], was also formulated in superconductivity and nuclear dynamics. In this study, we formulate the TDHFB method for molecular systems as a simple method for calculating excited states that can consider static electron correlations.

The two methods for solving the TD equation are time- and frequency-domains. The frequency-domain method, based on the Casida equation[37], has been popular in quantum chemistry because the excitation energy and associated transition moment are the most significant properties. Meanwhile, the time-domain method, called the real-time (RT) method[38–42], is popular in nuclear physics because it enables observation of the time evolution of a state. In addition, its computational cost is formally lower than that of the frequency-domain method [43]. Almost all previous studies in nuclear physics have solved the TDHFB equation using the RT method. Therefore, we applied the RT method and developed RT-TDHFB to obtain excited-state information.

The RT-TDHFB method has the disadvantage that the HFB wavefunction is not necessarily an eigenfunction of the number operator; therefore, the electron number can change during time evolution. To avoid this change, we focus on applying the canonical basis (Cb)-TDHFB method developed in nuclear physics to nuclear dynamics calculations[44–46]. This method introduces a TD canonical basis that diagonalizes the density matrix at any time and approximates the pairing field matrix in diagonal form. Accordingly, the expectation value of the electron number was conserved.

In this study, we tested the performance of the Cb-TDHFB method on the excited states of the H_2 molecules. Section II presents the RT-TDHFB and Cb-TDHFB formalisms after a summary of the HFB method. In Section III, we present the implementation of these RT/Cb-TDHFB schemes. In Section IV, the numerical calculations and analysis of hydrogen molecules are presented. Finally, we conclude the study in Section V.

II. Methods

A. Restricted closed-shell HFB theory

The HFB energy is expressed as a spin-orbital representation as follows [27]:

$$E_{\mathrm{HFB}} = \sum_{ij} h_{ij} D_{ji} + \frac{1}{2} \sum_{ijkl} (\langle ik|jl\rangle - \langle ik|lj\rangle) D_{ji} D_{lk} - \frac{1}{4} \zeta \sum_{ijkl} (\langle ij|kl\rangle - \langle ij|lk\rangle) K_{ij}^{*} K_{kl} \qquad (1)$$

where h_{ij} is the ijth element of the one-electron integral matrix $\boldsymbol{h}$ and $\langle ij|kl\rangle = \iint \psi_i^*(r_1)\psi_j^*(r_2) r_{12}^{-1} \psi_k(r_1)\psi_l(r_2) dr_1 dr_2$ are the two-electron integrals for orbitals $\{\psi_i\}$. D_{ij} and K_{ij} are the ijth elements of the electron density matrix $\boldsymbol{D}$ and electron pairing matrix $\boldsymbol{K}$, respectively. The elements of

these matrices are expressed with the HFB wavefunction and electron creation and annihilation operators $a_i^\dagger$ and a_i, as

$$D_{ij} = \langle \Psi_{\mathrm{HFB}} | a_j^\dagger a_i | \Psi_{\mathrm{HFB}} \rangle = D_{ji}^* \tag{2}$$

$$K_{ij} = \langle \Psi_{\mathrm{HFB}} | a_j a_i | \Psi_{\mathrm{HFB}} \rangle = -K_{ji} \tag{3}$$

and the third term in Eq. (1) represents the pair energy, which effectively considers static correlation, and ζ is a tunable parameter that describes the magnitude of the static correlation introduced by Scuseria[27].

In this study, we focused only on the spin-restricted closed-shell case (i.e., RHFB[47]). In the RHFB method, $\boldsymbol{D}$ and $\boldsymbol{K}$ satisfy the following relationship:

$$\overline{\boldsymbol{D}} \equiv \boldsymbol{D}^{\alpha\alpha} = \boldsymbol{D}^{\beta\beta}, \tag{4}$$

$$\boldsymbol{D}^{\alpha\beta} = \boldsymbol{D}^{\beta\alpha} = \boldsymbol{0}, \tag{5}$$

$$\overline{\boldsymbol{D}}^\dagger = \overline{\boldsymbol{D}}, \tag{6}$$

$$\overline{\boldsymbol{K}} \equiv \boldsymbol{K}^{\alpha\beta} = -\boldsymbol{K}^{\beta\alpha}, \tag{7}$$

$$\boldsymbol{K}^{\alpha\alpha} = \boldsymbol{K}^{\beta\beta} = \boldsymbol{0}, \tag{8}$$

$$\overline{\boldsymbol{K}}^{\mathrm{T}} = \overline{\boldsymbol{K}}. \tag{9}$$

Then, the RHFB energy is written with spatial orthogonal orbitals:

$$E_{\mathrm{RHFB}} = 2 \sum_{ij}^{\mathrm{spatial}} h_{ij} \overline{D}_{ji} + \sum_{ijkl}^{\mathrm{spatial}} (2\langle ik|jl\rangle - \langle ik|lj\rangle) \overline{D}_{ji} \overline{D}_{lk}$$
$$-\zeta \sum_{ijkl}^{\mathrm{spatial}} \langle ij|kl\rangle \overline{K}_{ij} \overline{K}_{kl} + 2\Lambda \left(N - \sum_{i}^{\mathrm{spatial}} \overline{D}_{ii} \right), \tag{10}$$

where Λ is the chemical potential that conserves the average of the electron number.

In the RHFB formalism, the generalized density matrix $\boldsymbol{R}$ can be used, which is expressed in the case of an orthogonal basis set as

$$\overline{\boldsymbol{R}} = \begin{pmatrix} \overline{\boldsymbol{D}} & \overline{\boldsymbol{K}} \\ \overline{\boldsymbol{K}} & \mathbf{1} - \overline{\boldsymbol{D}} \end{pmatrix}. \tag{11}$$

Note that the following equation can be derived from the idempotency of $\overline{\boldsymbol{R}}$:

$$(\overline{\mathbf{K}})^2 = \overline{\mathbf{D}}(\mathbf{1} - \overline{\mathbf{D}}). \tag{12}$$

The energy variation in Eq. (10) with respect to $\overline{\boldsymbol{D}}$ and $\overline{\boldsymbol{K}}$ yields the following mean-field Hamiltonian matrix:

$$\boldsymbol{H} = \begin{pmatrix} \widetilde{\boldsymbol{F}} & \boldsymbol{\Delta} \\ \boldsymbol{\Delta} & -\widetilde{\boldsymbol{F}} \end{pmatrix}, \tag{13}$$

where $\widetilde{\boldsymbol{F}}$ is the shifted Fock matrix that represents the electron mean-field

$$\tilde{F}_{ij} = \frac{\partial E_{\mathrm{HFB}}}{\partial \overline{D}_{ji}} = h_{ij} - \Lambda\delta_{ij} + \sum_{kl}^{\text{spatial}} (2\langle ik|jl\rangle - \langle ik|lj\rangle)\overline{D}_{lk}\,, \tag{14}$$

and $\boldsymbol{\Delta}$ is the pairing-field matrix representing the quasiparticle mean field

$$\Delta_{ij} = \frac{\partial E_{\mathrm{HFB}}}{\partial \overline{K}_{ij}} = -\zeta \sum_{kl}^{\text{spatial}} \langle ij|kl\rangle \overline{K}_{kl}\,. \tag{15}$$

From Eq. (1), the pairing energy, which is the energy of static electron correlation, can also be expressed using the pairing matrix and the pairing field matrix as follow:

$$E_{pair} = \mathrm{Tr}(\mathbf{K}^*\boldsymbol{\Delta}) = \mathrm{Tr}(\mathbf{K}\boldsymbol{\Delta}^*). \tag{16}$$

However, when using a real orthogonal basis, it is simply a trace of the product of the pairing matrix and the pairing field matrix.

The quasiparticle orbital energies and their coefficients were obtained by solving the following HFB equation:

$$\begin{pmatrix} \widetilde{\boldsymbol{F}} & \boldsymbol{\Delta} \\ \boldsymbol{\Delta} & -\widetilde{\boldsymbol{F}} \end{pmatrix} \begin{pmatrix} \boldsymbol{X_i} \\ \boldsymbol{Y_i} \end{pmatrix} = -\begin{pmatrix} \boldsymbol{X_i} \\ \boldsymbol{Y_i} \end{pmatrix} \varepsilon_i. \tag{17}$$

Only half of the solutions with negative eigenvalues are used for the Bogoliubov transformation, leading to the following $\overline{\boldsymbol{D}}$ and $\overline{\boldsymbol{K}}$:

$$\overline{D}_{ij} = \sum_{k}^{M} Y_{ik}\, Y_{jk}, \tag{18}$$

$$\overline{K}_{ij} = \sum_{k}^{M} X_{ik}\, Y_{jk}, \tag{19}$$

where M denotes the number of quasiparticle orbitals. Note that the HFB wavefunction conserves the spatial and spin symmetries, but violates the particle-number symmetry. That is, the HFB wavefunction is not the eigenfunction of the number operator, but rather a superposition of different particle number determinants,

$$|\Psi_{\mathrm{HFB}}\rangle = \sum_{N} c_N\, |N\rangle, \tag{20}$$

where N is the particle number and $|N\rangle$ is the N-particle wavefunction. Therefore, the chemical potential in Eq. (10) was introduced to adjust the average number of electrons in the wavefunction to the correct value N.

B. RT-TDHFB theory

The TD HF/KS equation for a given TD potential for an external field, $V^{\mathrm{ext}}(\boldsymbol{r}, t)$, is expressed as the following:

$$i\frac{\partial}{\partial t}\psi_m(\boldsymbol{r}, t) = \left(\hat{F}(t) + \hat{V}^{\mathrm{ext}}(\boldsymbol{r}, t)\right)\psi_m(\boldsymbol{r}, t), \tag{21}$$

where $\hat{F}(t)$ is the TD Fock operator and $\hat{V}^{\mathrm{ext}}$ represents the interaction between the electron and the external field. This equation can be reformulated using the TD density matrix $\boldsymbol{D}(t)$:

$$i\frac{\partial}{\partial t}\boldsymbol{D}(t) = [\boldsymbol{F}(t) + \boldsymbol{V}^{\mathrm{ext}}(t), \boldsymbol{D}(t)]. \tag{22}$$

In the RT method, this equation was solved by directly integrating the time variable.

Here, we applied the RT method to solve the TDHFB equation[21], which can be expressed using the density matrix form as

$$i\frac{\partial}{\partial t}\overline{\boldsymbol{R}}(t) = [\boldsymbol{H}'(t), \overline{\boldsymbol{R}}(t)], \tag{23}$$

$$\boldsymbol{H}'(t) = \boldsymbol{H}(t) + \boldsymbol{V}^{\mathrm{ext}}(t), \tag{24}$$

where $\overline{\boldsymbol{R}}(t)$ and $\boldsymbol{H}(t)$ are the generalized density matrix and quasiparticle Hamiltonian, respectively, at time *t*. The TD generalized density matrix $\overline{\boldsymbol{R}}(t)$ comprises static and induced parts in terms of the external field.

$$\overline{\boldsymbol{R}}(t) = \overline{\boldsymbol{R}}^{(0)} + \delta\overline{\boldsymbol{R}}(t) = \overline{\boldsymbol{R}}^{(0)} + \sum_{n=1}^{\infty}\delta\overline{\boldsymbol{R}}^{(n)}(t)\,. \tag{25}$$

Similarly, the quasiparticle Hamiltonian is expressed as the sum of the static part corresponding to $\overline{\boldsymbol{R}}^{(0)}$ and the parts induced by $\delta\overline{\boldsymbol{R}}(t)$ as

$$\boldsymbol{H}(t) = \boldsymbol{H}^{(0)} + \delta\boldsymbol{H}(t) = \boldsymbol{H}^{(0)} + \sum_{n=1}^{\infty}\delta\boldsymbol{H}^{(n)}(t)\,. \tag{26}$$

In this study, we focus on the linear-response case:

$$i\frac{\partial}{\partial t}\delta\overline{\boldsymbol{R}}^{(1)}(t) = \left[\boldsymbol{H}^{(0)}, \delta\overline{\boldsymbol{R}}^{(1)}(t)\right] + \left[\delta\boldsymbol{H}^{(1)}(t), \overline{\boldsymbol{R}}^{(0)}\right] + \left[\boldsymbol{V}^{\mathrm{ext}}(t), \overline{\boldsymbol{R}}^{(0)}\right]. \tag{27}$$

Note that the nonlinear equation is also soluble using the RT-TDHFB method.

C. Canonical-basis TDHFB method

Because the ground-state HFB wavefunction is not the eigenfunction of the number operator, the RT-TDHFB method suffers from the fluctuation of the electron number during time evolution. Ebata *et al.*[44]

introduced a TD canonical basis into the RT-TDHFB theory in nuclear physics. In the resulting Cb-TDHFB method, TD canonical orbitals are obtained each time by diagonalizing the TD density matrix $\bar{\boldsymbol{D}}(t)$. This method can avoid the fluctuation of the electron number during time evolution. Note that this definition of the "canonical" orbital does not mean the orbitals that diagonalize the effective Hamiltonian such as canonical HF orbitals, but is similar to the "natural orbitals" in quantum chemical terminology.

The TD canonical orbital is defined by

$$i\frac{\partial}{\partial t}\psi'_m(\boldsymbol{r},t) = \left(\hat{F}(t) + \hat{V}^{\mathrm{ext}}(\boldsymbol{r},t)\right)\psi'_m(\boldsymbol{r},t), \tag{28}$$

where $\psi'_m(\boldsymbol{r},t)$ is the TD canonical molecular orbital and is represented by the MO expansion coefficient $\boldsymbol{C}(t)$

$$\psi'_m(\boldsymbol{r},t) = \sum_j C_{mj}(t)\chi_j(\boldsymbol{r}). \tag{29}$$

This coefficients matrix diagonalizes the density matrix:

$$\boldsymbol{C}^{\dagger}(t)\boldsymbol{D}(t)\boldsymbol{C}(t) = \begin{pmatrix} n_1(t) & \cdots & 0 \\ \vdots & \ddots & \vdots \\ 0 & \cdots & n_k(t) \end{pmatrix}. \tag{30}$$

The time evolution of the TD canonical orbitals is given by

$$i\frac{\partial}{\partial t}\boldsymbol{C}(t) = \boldsymbol{F}(t)\boldsymbol{C}(t) - \boldsymbol{C}(t)\boldsymbol{\eta}(t), \tag{31}$$

where $\boldsymbol{\eta}(t)$ is the gauge that makes the density matrix invariant to the orbital transformation and $\boldsymbol{\eta}(t)$ is the diagonal matrix with diagonal elements of the Fock matrix:

$$\eta_k(t) = \langle\phi_k|\hat{F}(t)|\phi_k\rangle. \tag{32}$$

We rewrite the TDHFB equation in the form of a time evolution equation for the density and pair matrices:

$$i\frac{\partial}{\partial t}\bar{\boldsymbol{D}}(t) = [\boldsymbol{F}(t), \bar{\boldsymbol{D}}(t)] + \bar{\boldsymbol{K}}(t)\boldsymbol{\Delta}^*(t) - \boldsymbol{\Delta}(t)\bar{\boldsymbol{K}}^*(t), \tag{33}$$

$$i\frac{\partial}{\partial t}\bar{\boldsymbol{K}}(t) = \boldsymbol{F}(t)\bar{\boldsymbol{K}}(t) + \bar{\boldsymbol{K}}(t)\boldsymbol{F}^*(t) + \boldsymbol{\Delta}(t)[\mathbf{1} - \bar{\boldsymbol{D}}^*(t)] - \bar{\boldsymbol{D}}(t)\boldsymbol{\Delta}(t). \tag{34}$$

Note that the pairing matrix at $t = 0$ is also diagonal according to Eq. (12). In addition, by approximating the pair potential to be diagonal:

$$\Delta_k(t)\delta_{kl} = \Delta_{kl}(t). \tag{35}$$

The equations for the diagonal elements of the density and pair matrices were derived from Eqs. (33) and (34).

$$i\frac{\partial}{\partial t}\bar{D}_k(t) = \bar{K}_k(t)\Delta_k^*(t) - \bar{K}_k^*(t)\Delta_k(t), \tag{36}$$

$$i\frac{\partial}{\partial t}\bar{K}_k(t) = 2\eta_k(t)\bar{K}_k(t) + \Delta_k(t)[2\bar{D}_k(t) - 1]. \tag{37}$$

Eq. (36) is the time evolution equation for the occupation number of time-dependent natural orbitals. In the usual Cb-TDHF equation, the number of occupancies does not change with time evolution and is either 2 or 0 (occupied or unoccupied). In the TD-DMFT, it is known that this time variation of the occupation number is necessary to describe correctly states in which two-electron excitations are predominant[36]. Since the right-hand side of Eq. (36) is the product of the diagonal components, the sum over k of the first and second terms is equal to the trace of the product of the pairing matrix and the pairing field matrix, respectively.

$$\sum_k \bar{K}_k(t)\Delta_k^*(t) = \mathrm{Tr}(\mathbf{K}\boldsymbol{\Delta}^*) \tag{38}$$

$$\sum_k \bar{K}_k^*(t)\Delta_k(t) = \mathrm{Tr}(\mathbf{K}^*\boldsymbol{\Delta}) \tag{39}$$

Assuming that the pairing energy remains constant during time evolution, the sum over k on the right-hand side of Eq. (36) is zero.

$$\mathrm{Tr}(\mathbf{K}(t)\boldsymbol{\Delta}^*(t)) = \mathrm{Tr}(\mathbf{K}^*(t)\boldsymbol{\Delta}(t)) \tag{40}$$

Hence, the trace of the density matrix, i.e., the number of electrons, is also constant during time evolution.

In addition to Eqs. (36) and (37), the time evolution equation of the canonical orbital in Eq. (31) is solved by numerical integration.

III. Implementation

We implemented RT-TDHFB and Cb-TDHFB codes in the GAMESS program[48]. The following is the procedure of the Cb-TDHFB method:

[1] The HFB wavefunction in the ground state is calculated to obtain the static generalized density and Hamiltonian.

[2] The canonical basis set is constructed by diagonalizing the density matrix. The pairing matrix was transformed using a canonical basis. Off-diagonal elements of the pairing-field matrix is discarded.

[3] The new canonical basis function, diagonal density, and pairing matrices under an external field are updated using Eqs. (31), (36), and (37). We adopted the fourth-order Runge–Kutta method for numerical integration. The potential of the applied external field is given by

$$V_{ij}^{\mathrm{ext}}(t) = \varepsilon(t)\mathbf{e}^{\mathrm{ext}} \cdot \langle \phi_i | \boldsymbol{r} | \phi_j \rangle, \tag{41}$$

where $\mathbf{e}^{\mathrm{ext}}$ is a unit vector of the external field, $\langle \phi_i | \boldsymbol{r} | \phi_j \rangle$ is the dipole integral, and $\varepsilon(t)$ represents the TD part of the external field. In this study, we adopted a delta-function-type external field:

$$\varepsilon(t) = \delta(t). \tag{42}$$

[4] The induced polarization of the electrons at each time step is calculated:

$$\delta \boldsymbol{P}(t) = -\sum_{ij} \delta \overline{D}_{ij}(t) \langle \phi_j | \boldsymbol{r} | \phi_i \rangle. \quad (43)$$

[5] The absorption spectrum is obtained from the time variation of the induced polarization through Fourier transform (FT) analysis.

Note that only states with non-zero dipole transition moments are obtained as excited states since this study employed a dipole-type operator.

IV. Numerical Application

In this section, we present the numerical results obtained using the TDHFB method. We applied the RT/Cb-TDHFB method to H_2 molecules. In the TDHFB calculation, we set ζ, which is a parameter of the HFB method, to 1.0, in all cases. In the time evolution, we adopted the direction of the external fields, $\mathbf{e}^{\mathrm{ext}} = (1,1,1)$ in all calculations. All time evolutions were run over T = 8.0 fs with a time interval of Δt = 0.48 as (0.02 a.u. of time). Therefore, the resolution of the absorption spectrum ΔE is 0.52 eV from the uncertainty principle $\Delta E \sim h/T$, where h is the Planck constant and T is the simulation time.

Throughout this study, we adopted the correlation-consistent polarized valence double-ζ (cc-pVTZ) basis set unless otherwise stated.

A. Ground state

Fig. 1 shows the potential energy curves for the H_2 molecule. Around the equilibrium bond length where the static correlation is sufficiently small, the HFB energy coincides with the RHF energy. In contrast, the

HFB results qualitatively describe the bond dissociation curve. However, because the HFB method overestimates the static correlation, the HFB energy becomes lower than the full CI energy. If the parameter ζ was adopted as 0.8, the HFB potential curve was almost parallel to the full CI potential curve.

B. RT-TDHFB calculation

First, we performed the RT-TDHFB calculation of the H_2 molecule at the equilibrium bond length (r = 0.75 Å), where the static correlation is sufficiently small. Fig. 2 (upper) show the time evolution of the induced polarization $\delta\boldsymbol{P}^{(1)}(t)$ and the absorption spectrum obtained from the FT analysis of $\delta\boldsymbol{P}^{(1)}(t)$. For comparison, the results of the RT-TDHF calculations are shown in Fig. 2 (lower). In this simple weak-correlation case, the RT-TDHFB results coincided with the RT-TDHF results.

As a stretched bond (r = 2.6 Å), the results changed, as shown in Fig. 3. Note that the RT-TDHF results are qualitatively inadequate because it is a spin-restricted formalism. The oscillation of the induced polarization by the RT-TDHFB calculation is approximately one order of magnitude larger than that by the RT-TDHF calculation. Accordingly, many unphysical peaks appear in the absorption spectrum, especially in the high-energy regions. Fig. 4(a) shows the fluctuation of the expectation value of the electron number during the time evolution in the RT-TDHFB calculation compared with the RT-TDHF calculation. Fig. 4(b) shows the FT analysis of the electron number fluctuation. Strong peaks are observed in the high-energy regions, which correspond to the absorption spectrum. Therefore, the change in the electron number affects the induced

polarization in the RT-TDHFB calculation. Furthermore, dependence of the fluctuation on the time step used in the time evolution (Δt) is investigated in Fig. S3 in Supplementary Materials.

C. Canonical-basis TDHFB calculation.

We performed the Cb-TDHFB calculations for the H_2 molecule. In the equilibrium bond length (r = 0.75 Å), the Cb-TDHFB results depicted in Fig. S1 coincide with the RT-TDHF results as well as the RT-TDHFB ones.

As the H-H bond is stretched (r = 2.6 Å), the results changed, as shown in Fig. 5. As for the electron number, the Cb-TDHFB method could suppress the change in the electron number during the time evolution (Fig. S2). This indicates that the polarization and absorption spectra in the Cb-TDHFB calculation can eliminate the effect of the electron number change. Table I compares the excitation energies of the Cb-TDHFB, RT-TDHF, and full CI calculations for the H_2 molecule (r = 2.6 Å). The Σ_u^+ states appear as excitations in the z direction in the Cb-TDHFB calculation. In the low energy region ($\leq$10 eV), the Cb-TDHFB results are not consistent with those of full CI. However, at high energy region ($>$15 eV), the Cb-TDHFB energies accurately reproduce the full-CI ones. The Π_u state appears as an excitation in the x and y directions, and the excitation energy and oscillator strength by the Cb-TDHFB method also correspond to those of full CI. The other states, which are not dipole-allowed, do not appear in excited state calculations using real-time methods. We also performed Cb-TDHFB calculations for an LiH molecule in Supplementary Materials. We found as

well as for the H_2 molecule, i.e., the high-energy region is described correctly, whereas the low-energy region is described poorly (Fig. S4).

The TDHFB method equips with a time evolution equations not only for the natural orbitals but also for the occupation numbers, suggesting a connection with TD-DMFT. Previous studies have shown that TD-DMFT can correctly describe two-electron excited states missing in the TD-DFT[35,36]. In a hydrogen molecule, this state is a totally symmetric representation. However, this state does not appear in the Cb-TDHFB calculation because it does not have a transition moment. We consider that these states can be treated if we formulate the Cb-TDHFB method in the Casida-like equation as well as the TD-DMFT, but the present Cb-TDHFB calculation includes doubly excited configurations in the ground state, and it can obtain one-electron excited states from such configurations.

D. Hartree–Fock orbital analysis

In this study, we analyzed the absorption spectrum using canonical HF orbitals. First, the TDHFB density matrix is projected onto a static canonical HF orbital basis. Note that the canonical HF orbitals were constructed separately from the HFB calculations for analysis. Although the occupation numbers of the canonical HF orbitals are zero or two for the RHF density matrix, these canonical orbitals are fractionally occupied for the HFB density matrix. Therefore, excitation from the orbital, which is virtual in the RHF, but partially occupied in the HFB, can occur. The time variation of the density matrix in the canonical HF orbital basis provides a transition based on the HF canonical orbital. For example, matrix

elements $D_{ij}(t)$ correspond to the TD interaction between canonical HF orbitals *i* and *j*. FT analysis of the time variation $D_{ij}(t)$ gives us a spectrum

$$D_{ij}(\omega) = \int_{-\infty}^{\infty} D_{ij}(t)\, e^{-i\omega t}. \tag{44}$$

Then, the spectrum was compared with the absorption spectrum to assign the nature of the transition based on the HF canonical orbitals. We applied this analysis to the results of the Cb-TDHFB calculation of the stretched H_2 molecule with r = 2.6 Å. Figure 6 (b) shows the spectrum of the canonical HF orbital analysis of Eq. (44). For simplicity, we used the 6-31G basis set. Fig. 6 (a) shows the canonical HF orbitals and their occupation numbers in the ground-state HFB wavefunction. The spectrum of the RT-TDHF results is shown in Fig. 6 (c). For parity symmetry, D_{13} and D_{24} were zero. The Cb-TDHFB result has non-zero components that are not relevant to MO1, which do not appear in the RT-TDHF result where only MO1 is occupied. In the first and second excited states (i.e., 1.6 and 2.6 eV), the transition of MO1 and MO2 (D_{12}) is dominant, but that between MO1 and MO4 (D_{14}) also exists. A similar contribution was observed for the first excited state (4.1 eV) of the RT-TDHF sample. Note that, in the case of the Cb-TDHFB result, the D_{12} contribution may include the electron transition from MO2 to MO1, as well as that from MO1 to MO2. In addition, transitions between MO2 and MO3 (D_{23}) and between MO3 and MO4 (D_{34}) exist in the Cb-TDHFB results. It is because that the ground state wavefunction of the HFB method has a multiconfigurational character. For comparison, the full CI wave functions and excitation energies are summarized in Table II. The first excitation energy by the full CI method is 10.05 eV, indicating that the energy by the Cb-TDHFB method is estimated to be lower. $S_1 \leftarrow S_0$ excitation in the full CI method can be approximated as transitions from MO1 to MO2

($\Phi_{11}\rightarrow\Phi_{12}/\Phi_{21}$), MO2 to MO1 ($\Phi_{22}\rightarrow\Phi_{12}/\Phi_{21}$), MO1 to MO4 ($\Phi_{11}\rightarrow\Phi_{14}/\Phi_{41}$), and MO2 to MO3 ($\Phi_{22}\rightarrow\Phi_{23}/\Phi_{32}$). Therefore, the transition analysis for the Cb-TDHFB results was consistent with the full-CI result.

In the third excited state (27.4 eV), the transition of D_{23} mainly contributed to the spectrum, although the D_{14} and D_{34} transitions also contributed to this state. However, only the D_{14} transition contributed to the second state (30.5 eV) in the RT-TDHF result. In the full CI result, this state corresponds to $S_4\leftarrow S_0$ excitation (26.38 eV) and can be approximated as transitions from MO2 to MO3 ($\Phi_{22}\rightarrow\Phi_{23}/\Phi_{32}$) and from MO1 to MO4 ($\Phi_{11}\rightarrow\Phi_{14}/\Phi_{41}$). This result is consistent with the Cb-TDHFB results, indicating that the Cb-TDHFB method can qualitatively describe the static correlation in the excited state. However, the accuracy of low-energy excited states is poor. This is probably because these peaks originate from the breakdown of number symmetry, called the Nambu–Goldstone mode in nuclear physics[49,50].

V. Conclusion

In this study, the TDHFB method was applied to molecular systems to treat excited states with large static correlations at a reasonable computational cost. We first developed the RT-TDHFB method by combining the real-time propagation method with the HFB wavefunction, which can describe static correlation. Around the equilibrium structure of the H_2 molecule, where the static correlation is weak, the RT-TDHFB result is identical to the RT-TDHF result because the HFB ground state coincides with the HF ground state. In the structure with stretched bond, the RT-TDHFB result indicate many unphysical peaks in its absorption

spectrum that originate from violation of the total electron number. To avoid this, we adopted the Cb-TDHFB, which introduces the TD canonical basis and the diagonal approximation of the pairing field matrix to preserve the electron number. The Cb-TDHFB method successfully suppressed the fluctuation of the electron number and provided an absorption spectrum that was free from electron number changes. Projection onto the canonical HF orbitals provides the origin of the absorption peaks. We confirmed that the Cb-TDHFB method can qualitatively treat the ground and excited states with static electron correlation. However, the Cb-TDHFB results underestimated the excitation energies and generated spurious peaks around the low-energy region.

Although the Cb-TDHFB method conserves the average electron number, it is not an eigenfunction of the number operator. To recover the number symmetry, we will attempt the projection scheme[12] in the future.

Acknowledgments

Some of the present calculations were performed using computer facilities at the Research Center for Computational Science, Okazaki (Project:22-IMS-C019), and at the Research Institute for Information Technology, Kyushu University, Japan. This work was partially supported by JSPS KAKENHI Grant Number JP17K05738 and the Photo-excitonix Project of Hokkaido University. M. N. would like to thank the Hokkaido University Ambitious Doctoral Fellowship (Information Science/AI) from MEXT. TA was supported by a Research Fellowship for Young Scientists from the Japan Society for the Promotion of Science (JSPS). The Institute for Chemical Reaction Design and Discovery (ICReDD) was established by the World

Premier International Research Initiative (WPI), Ministry of Education, Culture, Sports, Science and Technology (MEXT), Japan. We would like to thank Editage (www.editage.com) for English language editing.

References

[1] B.O. Roos, The complete active space self-consistent field method and its applications in electronic structure calculations, Adv. Chem. Phys. 69 (1987) 399–445. https://doi.org/10.1002/9780470142943.ch7.

[2] B.O. Roos, R. Lindh, P.Å. Malmqvist, V. Veryazov, P.-O. Widmark, Multiconfigurational Quantum Chemistry, first ed, John Wiley & Sons, Ltd., 2016.

[3] R. Olivares-Amaya, W. Hu, N. Nakatani, S. Sharma, J. Yang, G.K.L. Chan, The ab-initio density matrix renormalization group in practice, J. Chem. Phys. 142 (2015) 034102. https://doi.org/10.1063/1.4905329.

[4] T. Yanai, M. Saitow, X.G. Xiong, J. Chalupský, Y. Kurashige, S. Guo, S. Sharma, Multistate complete-active-space second-order perturbation theory based on density matrix renormalization group reference states, J. Chem. Theory Comput. 13 (2017) 4829–4840. https://doi.org/10.1021/acs.jctc.7b00735.

[5] A. Baiardi, M. Reiher, The density matrix renormalization group in chemistry and molecular physics: Recent developments and new challenges, J. Chem. Phys. 152 (2020) 040903. https://doi.org/10.1063/1.5129672.

[6] C.J. Stein, M. Reiher, autoCAS: A program for fully automated multiconfigurational calculations, J. Comput. Chem. 40 (2019) 2216–2226. https://doi.org/10.1002/jcc.25869.

[7] P.R. Surján, An introduction to the theory of geminals, Top. Curr. Chem. 203 (1999) 63–88. https://doi.org/10.1007/3-540-48972-X_4.

[8] P.R. Surján, Geminal approach, in: Ref. Modul. Chem. Mol. Sci. Chem. Eng., Elsevier, 2016. https://doi.org/10.1016/b978-0-12-409547-2.11468-4.

[9] M. Tarumi, M. Kobayashi, H. Nakai, Accelerating convergence in the antisymmetric product of strongly orthogonal geminals method, Int. J. Quantum Chem. 113 (2013) 239–244. https://doi.org/10.1002/qua.24045.

[10] G.E. Scuseria, C.A. Jiménez-Hoyos, T.M. Henderson, K. Samanta, J.K. Ellis, Projected quasiparticle theory for molecular electronic structure, J. Chem. Phys. 135 (2011) 124108. https://doi.org/10.1063/1.3643338.

[11] V.A. Rassolov, A geminal model chemistry, J. Chem. Phys. 117 (2002) 5978–5987. https://doi.org/10.1063/1.1503773.

[12] V.A. Rassolov, F. Xu, S. Garashchuk, Geminal model chemistry II. Perturbative corrections, J. Chem. Phys. 120 (2004) 10385–10394. https://doi.org/10.1063/1.1738110.

[13] V.A. Rassolov, F. Xu, Geminal model chemistry III: Partial spin restriction, J. Chem. Phys. 126 (2007) 234112. https://doi.org/10.1063/1.2741266.

[14] V.A. Rassolov, F. Xu, Geminal model chemistry. IV. Variational and size consistent pure spin states, J. Chem. Phys. 127 (2007) 044104. https://doi.org/10.1063/1.2755738.

[15] P.A. Limacher, P.W. Ayers, P.A. Johnson, S. De Baerdemacker, D. Van Neck, P. Bultinck, A new mean-field method suitable for strongly correlated electrons: Computationally facile antisymmetric products of nonorthogonal geminals, J. Chem. Theory Comput. 9 (2013) 1394–1401. https://doi.org/10.1021/ct300902c.

[16] P.A. Johnson, P.W. Ayers, P.A. Limacher, S. De Baerdemacker, D. Van Neck, P. Bultinck, A size-consistent approach to strongly correlated systems using a generalized antisymmetrized product of nonorthogonal geminals, Comput. Theor. Chem. 1003 (2013) 101–113. https://doi.org/10.1016/j.comptc.2012.09.030.

[17] D. Peng, H. Van Aggelen, Y. Yang, W. Yang, Linear-response time-dependent density-functional theory with pairing fields, J. Chem. Phys. 140 (2014) 18A522. https://doi.org/10.1063/1.4867540.

[18] C. Bannwarth, J.K. Yu, E.G. Hohenstein, T.J. Martínez, Hole-hole Tamm-Dancoff-approximated density functional theory: A highly efficient electronic structure method incorporating dynamic and static correlation, J. Chem. Phys. 153 (2020) 024110. https://doi.org/10.1063/5.0003985.

[19] K. Pernal, K. Chatterjee, P.H. Kowalski, How accurate is the strongly orthogonal geminal theory in predicting excitation energies? Comparison of the extended random phase approximation and the linear response theory approaches, J. Chem. Phys. 140 (2014). https://doi.org/10.1063/1.4855275.

[20] M. Hapka, K. Pernal, H.J.A. Jensen, An efficient implementation of time-dependent linear-response theory for strongly orthogonal geminal wave function models, J. Chem. Phys. 156 (2022). https://doi.org/10.1063/5.0082155.

[21] J.P. Blaizot, G. Ripka, Quantum Theory of Finite Systems, MIT Press, 1986.

[22] P. Ring, P. Schuck, The Nuclear Many-Body Problem, third, Springer, 2004. https://link.springer.com/book/9783540212065 (accessed March 22, 2022).

[23] J.R. Schrieffer, Theory of super conductivity, Phys. Rev. 108 (2018) 1–332. https://doi.org/10.1201/9780429495700.

[24] A.J. Coleman, Structure of fermion density matrices. II. Antisymmetrized geminal powers, J. Math. Phys. 6 (1965) 1425–1431. https://doi.org/10.1063/1.1704794.

[25] W. Kutzelnigg, On the validity of the electron pair approximation for the Beryllium ground state, Theor. Chim. Acta. 3 (1965) 241–253. https://doi.org/10.1007/BF00527720.

[26] D.A. Mazziotti, Energy functional of the one-particle reduced density matrix: A geminal approach, Chem. Phys. Lett. 338 (2001) 323–328. https://doi.org/10.1016/S0009-2614(01)00251-2.

[27] V.N. Staroverov, G.E. Scuseria, Optimization of density matrix functionals by the Hartree-Fock-Bogoliubov method, J. Chem. Phys. 117 (2002) 11107–11112. https://doi.org/10.1063/1.1523060.

[28] G. Csányi, T. Arias, Tensor product expansions for correlation in quantum many-body systems, Phys. Rev. B - Condens. Matter Mater. Phys. 61 (2000) 7348–7352. https://doi.org/10.1103/PhysRevB.61.7348.

[29] K. Pernal, K.J.H. Giesbertz, Reduced density matrix functional theory (RDMFT) and linear response time-dependent RDMFT (TD-RDMFT), Top Curr Chem. (2016) 125–183. https://doi.org/10.1007/128_2015_624.

[30] T. Tsuchimochi, G.E. Scuseria, Strong correlations via constrained-pairing mean-field theory, J. Chem. Phys. 131 (2009) 121102. https://doi.org/10.1063/1.3237029.

[31] G.E. Scuseria, T. Tsuchimochi, Constrained-pairing mean-field theory. II. Exact treatment of dissociations to nondegenerate orbitals, J. Chem. Phys. 131 (2009) 164119. https://doi.org/10.1063/1.3257965.

[32] T. Tsuchimochi, G.E. Scuseria, A. Savin, Constrained-pairing mean-field theory. III. Inclusion of density functional exchange and correlation effects via alternative densities, J. Chem. Phys. 132 (2010) 024111. https://doi.org/10.1063/1.3292640.

[33] T. Tsuchimochi, T.M. Henderson, G.E. Scuseria, A. Savin, Constrained-pairing mean-field theory. IV. Inclusion of corresponding pair constraints and connection to unrestricted Hartree-Fock theory, J. Chem. Phys. 133 (2010) 134108. https://doi.org/10.1063/1.3490478.

[34] J.K. Ellis, C.A. Jiménez-Hoyos, T.M. Henderson, T. Tsuchimochi, G.E. Scuseria, Constrained-pairing mean-field theory. V. Triplet pairing formalism, J. Chem. Phys. 135 (2011) 034112. https://doi.org/10.1063/1.3610650.

[35] K.J.H. Giesbertz, E.J. Baerends, O. V. Gritsenko, Charge transfer, double and bond-breaking excitations with time-dependent density matrix functional theory, Phys. Rev. Lett. 101 (2008). https://doi.org/10.1103/PhysRevLett.101.033004.

[36] K.J.H. Giesbertz, K. Pernal, O. V. Gritsenko, E.J. Baerends, Excitation energies with time-dependent density matrix functional theory: Singlet two-electron systems, J. Chem. Phys. 130 (2009). https://doi.org/10.1063/1.3079821.

[37] M.E. Casida, M. Huix-Rotllant, Progress in time-dependent density-functional theory, Annu. Rev. Phys. Chem. 63 (2012) 287–323. https://doi.org/10.1146/annurev-physchem-032511-143803.

[38] K. Yabana, G.F. Bertsch, Time-dependent local-density approximation in real time, Phys. Rev. B. 54 (1996) 4484–4487.

[39] K. Yabana, T. Nakatsukasa, J.I. Iwata, G.F. Bertsch, Real-time, real-space implementation of the linear response time-dependent density-functional theory, Phys. Status Solidi Basic Res. 243 (2006) 1121–1138. https://doi.org/10.1002/pssb.200642005.

[40] T. Akama, H. Nakai, Short-time Fourier transform analysis of real-time time-dependent Hartree-Fock and time-dependent density functional theory calculations with Gaussian basis functions, J. Chem. Phys. 132 (2010) 054104. https://doi.org/10.1063/1.3300127.

[41] T. Akama, Y. Imamura, H. Nakai, Application of real-time time-dependent density functional theory with the CVB3LYP functional to core excitations, Chem. Lett. 39 (2010) 407–409. https://doi.org/10.1246/cl.2010.407.

[42] J.J. Goings, P.J. Lestrange, X. Li, Real-time time-dependent electronic structure theory, Wiley Interdiscip. Rev. Comput. Mol. Sci. 8 (2018) e1341. https://doi.org/10.1002/wcms.1341.

[43] C.Y. Yam, S. Yokojima, G.H. Chen, Linear-scaling time-dependent density-functional theory, Phys. Rev. B - Condens. Matter Mater. Phys. 68 (2003) 153105. https://doi.org/10.1103/PHYSREVB.68.153105.

[44] S. Ebata, T. Nakatsukasa, T. Inakura, K. Yoshida, Y. Hashimoto, K. Yabana, Canonical-basis time-dependent Hartree-Fock-Bogoliubov theory and linear-response calculations, Phys. Rev. C. 82 (2010) 034306. https://doi.org/10.1103/PhysRevC.82.034306.

[45] S. Ebata, T. Nakatsukasa, T. Inakura, Systematic investigation of low-lying dipole modes using the canonical-basis time-dependent Hartree-Fock-Bogoliubov theory, Phys. Rev. C - Nucl. Phys. 90 (2014) 024303. https://doi.org/10.1103/PhysRevC.90.024303.

[46] S. Ebata, Studies on nuclear structure and nuclear dynamics using Cb-TDHFB, Front. Phys. 8 (2020). https://doi.org/10.3389/fphy.2020.00102.

[47] M. Kobayashi, Gradient of molecular Hartree-Fock-Bogoliubov energy with a linear combination of atomic orbital quasiparticle wave functions, J. Chem. Phys. 140 (2014) 084115. https://doi.org/10.1063/1.4866796.

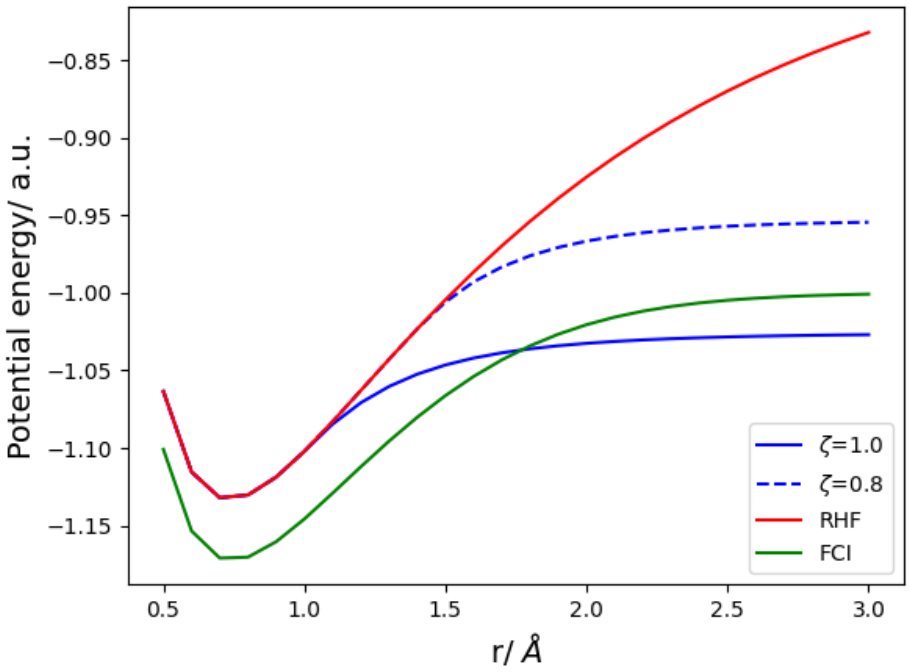
[48] M.W. Schmidt, K.K. Baldridge, J.A. Boatz, S.T. Elbert, M.S. Gordon, J.H. Jensen, S. Koseki, N. Matsunaga, K.A. Nguyen, S. Su, T.L. Windus, M. Dupuis, J.A. Montgomery, General atomic and

molecular electronic structure system, J. Comput. Chem. 14 (1993) 1347–1363. https://doi.org/10.1002/jcc.540141112.

[49] J. Goldstone, Field theories with “Superconductor” solutions, Nuovo Cim. 19 (1961) 154–164. https://doi.org/10.1007/BF02812722.

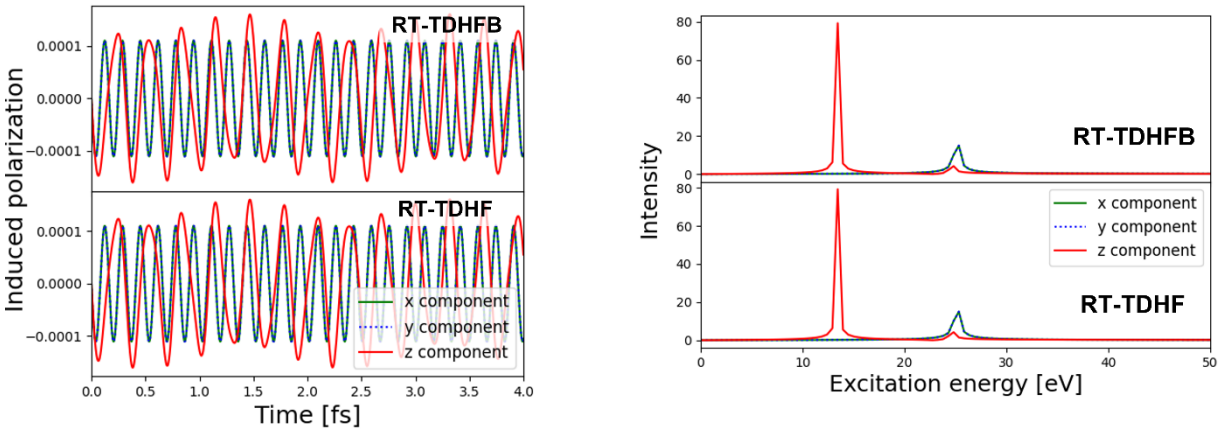
[50] P. Schuck, D.S. Delion, J. Dukelsky, M. Jemai, E. Litvinova, G. Röpke, M. Tohyama, Equation of motion method for strongly correlated fermi systems and extended RPA approaches, Phys. Rep. 929 (2021) 1–84. https://doi.org/10.1016/j.physrep.2021.06.001.

Artwork and Tables with captions



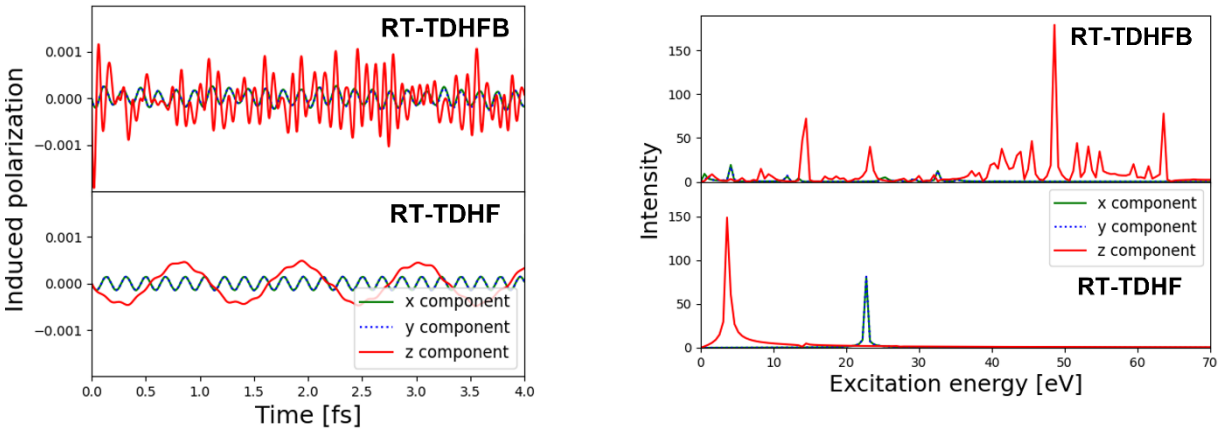
(single-column) Fig. 1. Potential energy curves for the H_2 molecule.

(a) (b)



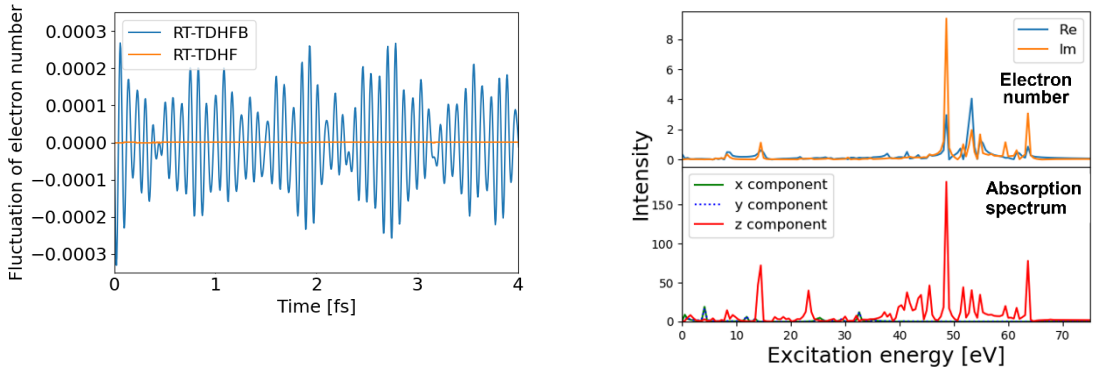
(2-column) Fig. 2. (a) Time variation of $\delta P^{(1)}(t)$ in H_2 (r=0.75 Å) and (b) absorption spectrum with (upper) RT-TDHFB and (lower) RT-TDHF methods.

(a) (b)



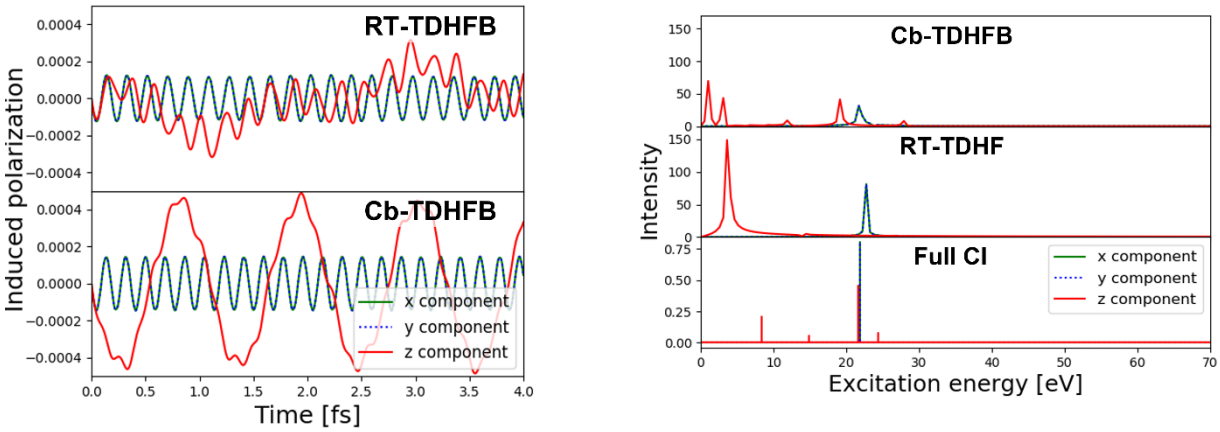
(2-column) Fig. 3. (a) Time variation of $\delta P^{(1)}(t)$ in H_2 (r=2.6 Å) and (b) absorption spectrum with (upper) RT-TDHFB and (lower) RT-TDHF methods.

(a) (b)

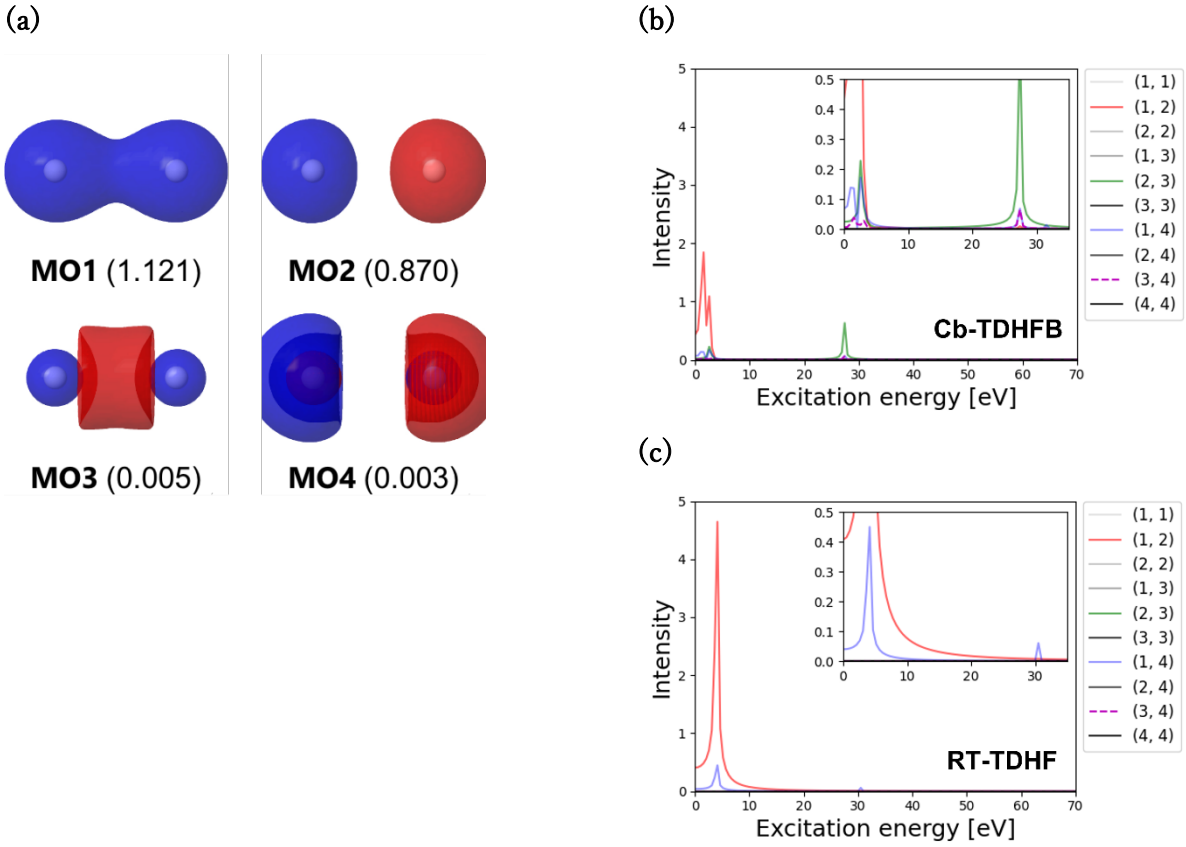


(2-column) Fig. 4. (a) Fluctuation of the electron number during the time evolution in the RT-TDHFB or RT-TDHF calculation of H_2 (r=2.6 Å) and (b) FT analysis of (upper) the electron number fluctuation and (lower) absorption spectrum in the RT-TDHFB calculation of H_2 (r=2.6 Å).

(a) (b)



(2-column) Fig. 5. (a) Time evolution of $\delta P^{(1)}(t)$ of H_2 (r=2.6 Å) with (upper) Cb-TDHFB and (lower) RT-TDHF methods. (b) Absorption spectrum with (upper) Cb-TDHFB, (middle) RT-TDHF, and (lower) full CI methods.



(2-coulmn) Fig. 6. HF orbital analysis of the spectrum in H_2 (r=2.6 Å). (a) Canonical HF orbital and occupation number in the parentheses. (b) Cb-TDHFB. (c) RT-TDHF.

Table I. Excitation energies $\hbar\omega$ of H_2 molecule (r=2.6 Å) obtained by the RT-TDHF, Cb-TDHFB, and full CI calculation using the cc-pVTZ basis.

Direction	RT-TDHF $\hbar\omega$ (eV)	Cb-TDHFB $\hbar\omega$ (eV)	Full CI $\hbar\omega$ (eV) /symmetry
z		1.00	
z	3.60	3.10	8.42 /Σ_u^+
z	14.50	11.90	14.91 /Σ_u^+
z		19.10	21.57 /Σ_u^+
x, y	22.70	21.70	21.93 /Π_u
z	27.90	27.90	24.38 /Σ_u^+

Table II. The full CI calculation in H_2 molecule with r = 2.6 Å using the 6-31G basis.

State	Excitation energy (eV)	Wavefunction
S_0	0.0	$0.787\Phi_{11} - 0.606\Phi_{22} + 0.061\Phi_{31} + 0.061\Phi_{13} + 0.055\Phi_{24} + 0.055\Phi_{42}$
S_1	10.05	$0.702\Phi_{12} + 0.702\Phi_{21} - 0.071\Phi_{32} - 0.071\Phi_{23} + 0.043\Phi_{34} + 0.043\Phi_{43} + 0.012\Phi_{41} + 0.012\Phi_{14}$
S_2	10.27	$0.780\Phi_{22} + 0.612\Phi_{11} - 0.081\Phi_{13} - 0.081\Phi_{31} - 0.055\Phi_{33} - 0.035\Phi_{44}$
S_3	25.91	$0.557\Phi_{31} + 0.557\Phi_{13} + 0.416\Phi_{42} + 0.416\Phi_{24} - 0.089\Phi_{44} + 0.067\Phi_{33} + 0.037\Phi_{11}$
S_4	26.38	$0.515\Phi_{32} + 0.515\Phi_{23} + 0.482\Phi_{41} + 0.482\Phi_{14} + 0.043\Phi_{21} + 0.014\Phi_{34}$